Journal of Polymer Research (2022) 29: 197
https://doi.org/10.1007/s10965-022-03050-1

ORIGINAL PAPER

Exploring cocatalyst type effect on the Ziegler–Natta catalyzed ethylene polymerizations: experimental and DFT studies

Maryam Masoori[1] · Mehdi Nekoomanesh[1] · Sergio Posada-Pérez[2] · Reza Rashedi[3] · Naeimeh Bahri-Laleh[1]

Received: 8 March 2022 / Accepted: 25 April 2022 / Published online: 5 May 2022

Abstract

Due to the important role of cocatalyst in the polymerization process employing industrially favored Ziegler–Natta catalysts, its effect on kinetic behavior, catalyst activity, and polymer properties is discussed. In this paper, triethyl aluminum (TEA) and triisobutyl aluminum (TIBA) have been used as the main cocatalyst ingredient with 10–20 mol percent of diethyl aluminum chloride (DEAC) and ethyl aluminum dichloride (EADC) cocatalysts, being neat TEA the cocatalysts with the highest activity. Moreover, TEA-DEAC and TEA-EADC cocatalysts revealed a built-up kinetic profile, while TIBA-DEAC and TIBA-EADC show a decay-type kinetic curve. According to melt flow index results, no considerable change in flowability was detected in the synthesized polyethylenes (PE). On the other hand, the ethylene insertion and chain termination mechanisms were investigated by means of density functional calculations using Ti active center located in (110) and (104) facets of the $MgCl_2$ surface. To shed light on the bulkiness level of employed cocatalysts, buried volume (V_{Bur}) together with the two-dimensional map of cocatalyst systems were considered. Higher V_{Bur} of TIBA complex can explain its lower activity and decay type kinetic profile obtained by experimental studies.

Keywords Ethylene polymerization · Ziegler–Natta catalyst · Polymerization kinetics · DFT simulations

Introduction

Nowadays, it can be boldly said that the production of polymers using Ziegler–Natta catalysts is the most common industrial process for plastics production [1, 2]. Metallocene catalysts are nearly four decades old. Although advanced companies such as Basell, Dow, Sabic, Mitsui, Sommito, Borealis, Exxon Mobile, and Inoe use metallocene catalysts to produce some polyolefin grades, still more than 70% of polyolefins are prepared by Ziegler–Natta type catalysts [3, 4]. It is well stablished that the most important parameter to control the final polymer properties is the catalyst [5, 6]. On the other hand, it is noticed that the nature of this important chemical is practically undeniable without the presence of an activator, i.e., the use of cocatalysts [7, 8]. Despite a large amount of research has been carried out in the catalysts structural studies and polymerization conditions, the effect of important factors such as electron donor, cocatalyst, and comonomer in the catalyst performance and polymerization process is not very well explored and understood [9]. In the past, it was hypothesized that the cocatalyst is a passive component that only has the function of removing impurities and alkylating the active catalytic centers at the beginning of the polymerization, without playing a specific role in the ongoing process. Nevertheless, owing to its primary role in switching the polymerization reaction, the effect of cocatalysts is one of the key factors for the process performance. Indeed, after the catalyst, the selection of the appropriate cocatalyst is the most important and effective parameter in olefin polymerization processes [10]. The type of cocatalyst not only affects catalyst productivity but also alters the microstructure and arrangement of monomers in polymer

✉ Sergio Posada-Pérez
sergio.posada@udg.edu

✉ Naeimeh Bahri-Laleh
n.bahri@ippi.ac.ir

[1] Department of Polymerization Engineering, Iran Polymer and Petrochemical Institute, Tehran, Iran

[2] Institut de Química Computacional I Catàlisi and Departament de Química, Universitat de Girona, c/ Maria Aurèlia Company 69, 17003 Girona, Catalonia, Spain

[3] Jam Petrochemical Company, Research and Development Department, South Pars Special Economic Zone, AsaluyehAsaluyeh, Iran

chains during the polymerization reaction [11, 12]. It is well-known that, in a polymerization process, the cocatalyst i) activates pre-catalyst particles, ii) participates in chain transfer reactions, iii) changes the isotacticity and molecular weight of the polymer [13], and iv) alters the kinetic stability and resistance to the decomposition of catalyst. According to the literature, different cocatalysts or their combinations cause different stability of the active centers with various performances which subsequently influence final properties of the polymer, including physical and mechanical properties [14].

Many studies have been focused on the catalyst structure, activity, polymerization, and properties of the polymer [15, 16], but only a few investigations have been carried out on the reactions and interactions of cocatalyst [17, 18]. The process of cocatalyst interaction with Ziegler–Natta catalysts is well understood, but the performance of different types of cocatalyst in these interactions is still unclear [19, 20]. Among the most common cocatalysts used in the commercial production of polyolefins are triethyl aluminum (TEA), triisobutyl aluminum (TIBA), diethyl aluminum chloride (DEAC), and ethyl aluminum dichloride (EADC). It is pointed out that such compounds, due to their various chemical structure, exhibit different behaviors in the olefin polymerizations. In fact, cocatalysts can form mono- and dimeric moieties, which indicates different capabilities toward pre-catalyst reduction/activation [21]. In addition to the type of cocatalyst, their concentration plays a relevant role. At lower cocatalyst concentrations, a large percentage of the primary catalyst remains inactive, and impurities and toxins are not removed appropriately. As a result, the consumption of the monomer increases dramatically, which is not economically affordable due to the high price of catalysts. Moreover, the high amount of cocatalyst (too optimal) causes excessive reduction of active catalytic centers and conversion of Ti^{3+} to Ti^{2+}. This leads to the lower activity of Ziegler–Natta catalyst in ethylene polymerizations and deactivation in propylene polymerizations [11, 22]. Owing to the fact that some cocatalysts like TEA have a positive effect on catalyst activity and chlorinate compounds like DEAC and EADC have a better ability to improve the product's properties, to investigate the polymerizations processes employing different cocatalysts combination is encouraged [23].

Due to the different behavior of the cocatalysts and knowing the fact that the new HDPE and LLDPE plants of Basell are based on the combination of TEA and TIBA with DEAC or EADC in low molar ratios of chlorinated cocatalysts, the efforts must be routed towards the investigation of cocatalysts combination. In this paper we thoroughly investigated the kinetics of catalyst behavior, and properties of the final polyethylene produced via a commercial $MgCl_2/TiCl_4$ based Ziegler–Natta catalyst in the presence of various cocatalysts including TEA, TIBA, and their combination with two chlorinated cocatalysts DEAC, EADC. Furthermore, density functional (DFT) approach were employed to shed light on the polyethylene chain formation in different $MgCl_2$ lateral cuts and alkylating capability of employed cocatalysts.

Experimental

Materials

Hydrogen gas (purity > 99%) as an active chain transfer agent was supplied from Roham Gas Company. An industrial $TiCl_4/MgCl_2$ based Ziegler–Natta catalyst, hexane as main medium in polymerization reactions, the polymerization grade of ethylene gas, were all acquired from Jam Company, Iran. Hexane was stored over a 4 Å activated molecular sieve. Triethylaluminium (TEA 1 M solution in hexane), triisobuthylaluminium (TIBA, 1 M solution in hexane), diethylaluminiumchloride (DEAC 1 M solution in hexane) and ethylaluminiumdichloride (EADC 1 M solution in hexane) as cocatalysts were purchased from Merck, Germany, and used as received.

Ethylene polymerization

In this study, all the operations were carried out in dry and oxygen free media under nitrogen flow. Polymerizations were carried out in stainless-steel setup equipped with a mechanical stirrer, high-pressure injection system, a pressure, and a temperature sensor. In order to prepare the reactor for polymerization, it was exposed to nitrogen for 1 h at 115 °C to remove impurities and moisture. After that, 650 mL of hexane was fed to the reactor at room temperature under nitrogen flow. After 3 min of degassing, the reactor was heated up to 80 °C at which cocatalyst (with a different molar ratio of cocatalyst combination) and catalyst were injected into the reactor. Then, 3 bar of hydrogen gas was fed, once a time, and the pressure was enhanced to 8 bar by ethylene monomer. The feeding of ethylene was continued to keep the total pressure at 8 bar (semi-batch polymerization process). After 2 h, the gases were completely vented, and the polymerization medium was cooled to room temperature. Finally, the polymer powder was dried at 85 °C.

Catalyst characterization

Scanning Electron Microscope (SEM): the catalyst morphology and distribution of elements on the surface of the catalyst was studied by SEM (VEGA TESCAN device made in Czechoslovakia) instrument. Inductively coupled plasma (ICP-MS): The magnesium and titanium contents of the employed catalyst were determined by ICP-MS. The power

of the ICP spectrometer (Varian 710-ES) was 1.10 kW. The flow rates of plasma gas and auxiliary gas were 15.0 and 1.50 L min^{-1}, respectively. The pressure of nebulizing gas was 200 kPa and the pump speed was 13 rpm. In this test, the catalyst was dissolved in hydrochloric acid to make an aqueous solution. Brunauer–Emmett–Teller (BET): Surface and pore analyses of the catalyst sample were done using the BET method (BELSORP Mini II). X-ray diffraction (XRD) of the catalyst was recorded using STOE-IPDS 2 T diffractometer employing graphite monochromatic Cu-Ka as electrode.

Polymer characterization

The melt flow index (MFI) of the synthesized polymers was measured using a Gottfert (MI-4) instrument. The polymer powders were mixed with 400 and 800 ppm of antioxidants (IRGANOX 1010, 168, respectively) before adding to the barrel. The MFI of powders was determined using ASTM D-1238 test method. The measurements were performed at 190 °C using 21.6, 5, and 2.16 kg loads, respectively.

Computational details

DFT calculations have been carried out with the Gausian16 [24] code using the BP86 functional of Becke and Perdew [25, 26], including corrections due to dispersion through the Grimme's method (GD3 keyword in Gaussian) [27]. The electronic configuration of the atoms has been described with the triple-ζ basis set with polarization of Ahlrichs for main-group atoms (def2-TZVP keyword in Gaussian) [28, 29]. The geometry optimizations were performed without symmetry constraints, and analytical frequency calculations confirmed the character of the located stationary points (only one negative frequency). These frequencies were used to calculate unscaled zero-point energies (ZPEs) as well.

Results and discussion

Characterization of catalyst

In the study of catalyst and polymerization process, the most basic task is to identify the structure, components, configuration, size, and size distribution of the catalyst. With a basic knowledge of the structure and chemistry of a catalyst, a good prediction of the behavior of the catalyst in the polymerization process can be provided. Table 1 shows the results of the structure and properties of the catalyst.

According to the Table 1 results, the catalyst had a Ti content of 2.4%, surface area of 243 m^2/g, average pore diameter of 3.97 nm and median particle size of 42.8 µm, which are accepted values for this class of systems. Furthermore, SEM picture, Fig. 1, revealed completely spherical morphology of employed catalyst, which is beneficial to the powder conveying in the industrial gas-phase reactors. According to the EDX analysis, beside Ti, Mg and Cl (which are main component of Ziegler–Natta catalyst), the catalyst contains considerable amount of C atom, that is mainly correlated to the presence of internal donor. Elemental mapping analysis implied that apart from Mg and Cl atoms that are representative of $MgCl_2$ support, Ti atom is also present in the structure of the catalyst. Moreover, uniform dispersion of Ti atoms indicated well stablished homogeneously dispersion of active sites on the $MgCl_2$ support structure.

The XRD spectrum of the catalyst in 2θ angles between 5 and 65° is illustrated in Fig. 2a. In this pattern, the peaks at 2θ angles of 14° (stacking of Cl–Mg–Cl triple layers along the crystallographic direction), 33° (corresponded to (104) plane) and 50° (corresponded to (110) plane) were detected [30]. According to the literature, highly disordered catalyst is usually obtained by the rotational disorder of Cl-Mg-Cl triple layers, which subsequently lead to the formation of classically considered surfaces, i.e. (104) and (110) facets

Table 1 Characterization of employed commercial catalyst

Catalyst	Ti[a]	Mg[b]	C[b]	Surf [c]	TPV[d]	APD[e]	D_avg[f]	X10[g]	X50[g]	X90[g]
	2.4[i] (2.7)[h]	13.3[i] (12.9)[h]	- (6.1)[h]	243	0.241	3.97	42.8	3.2	41.5	85.8

[a,b]weight percent (wt%)

[c]Surface area (m2/g)

[d]Total Pore Volume (Cm3/g)

[e]Average Pore Diameter (nm)

[f]Average dimension (µm)

[g]X10, X50 and X90 are the particle diameters at 10%, 50% and 90% in the cumulative number-base particle size distribution obtained by the LPS analysis

[h]the values were obtained from EDX analysis

[i]the values were obtained from ICP analysis

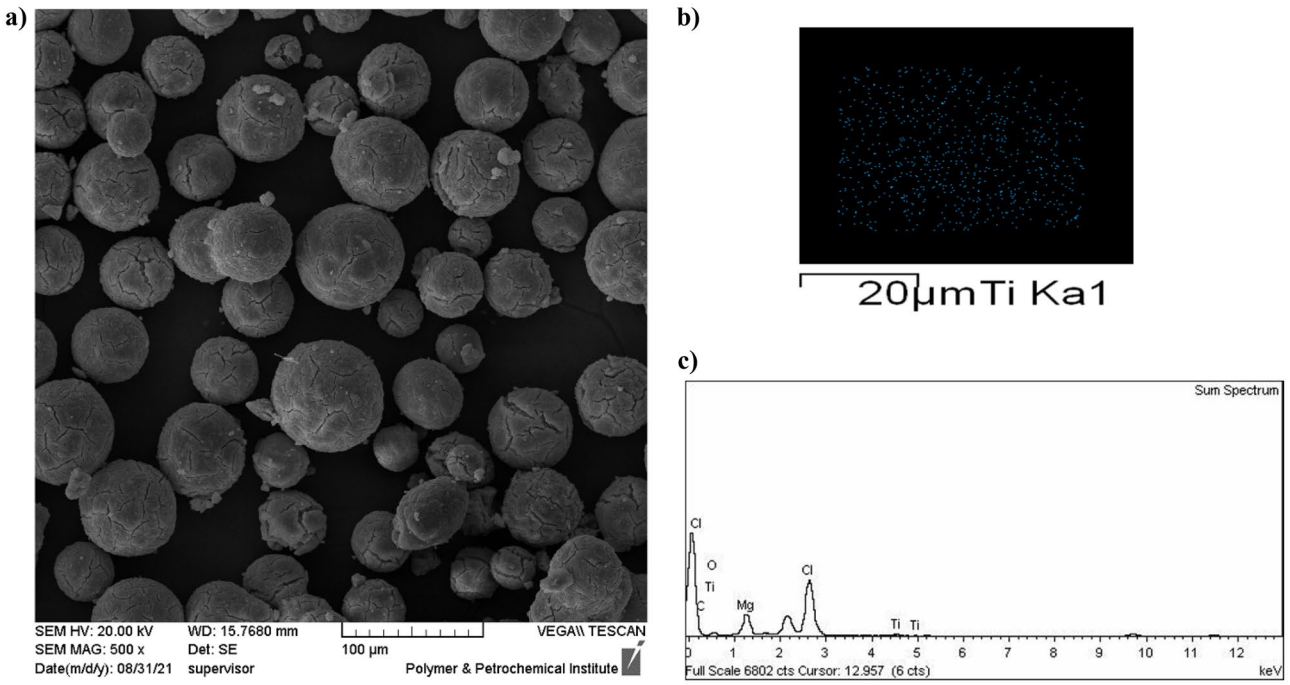

Fig. 1 **a** SEM, **b** Ti map and **c** EDX analyses of the employed catalyst

[6]. As can be seen in the XRD pattern, there is a small (0 0 3) peak and most of it slightly shifted to a smaller angle. According to the Wada et. al. [31] this shift can be attributed to the thin Cl-Mg-Cl layers (mostly < 10 layers). In another meaning, small peak of (003) layer, compared to neat $MgCl_2$ [32] (Fig. 2b), indicates that the crystallites in the employed catalyst contains 2–10 layers. Therefore, in building molecular structure of a Ziegler–Natta catalyst, these surfaces should be considered.

Ethylene polymerization in the presence of various cocatalysts

As mentioned, cocatalysts generally contain aluminum center, together with alkyl groups, chlorine atoms, etc., which based on their structure tune the performance of catalyst. Selecting the appropriate alkylaluminum complex can play a key role in the behavior of the catalyst, including polymerization activity, stereoselectivity, amount and distribution of active catalytic centers, as well as final characteristic of the polymer produced [4–8]. In this section, the polymerization behavior of employed Ziegler–Natta catalyst in the presence of various cocatalysts including TEA, TIBA, TEA + DEAC, TEA + EADC, TIBA + DEAC, and TIBA + EADC mixtures in different combinations of 90/10, 85/15, and 80/20, was surveyed in ethylene polymerization process.

For this purpose, in the constant molar ratio of Al/Ti = 200, the polymerization process was conducted in the presence of cocatalyst combinations under the same polymerization conditions. According to the results reported in Table 2, the catalyst activity was higher when TEA was used as cocatalyst, in comparison with TIBA. It can be attributed to the bulkiness of iso-buthyl groups which hinders its approaching to the Ti centers located in the interior parts of catalyst. By employing Cl containing Al complexes in the cocatalyst composition, EADC and DEAC, the activity was suppressed, although no clear trend was found between the amount of Cl-containing cocatalyst and its type with the catalyst activity.

In addition, the results reported in Table 2 show that the type of cocatalyst did not have a significant effect on the melt flow index. Although the polymers obtained in the presence of TIBA,TIBA/DEAC, and TIBA/EADC compared to TEA,TEA/DEAC, and TEA/EADC cocatalysts had lower melt flow index and narrower FRR, this difference was not large enough to be considered. Therefore, it can be said that the type and amount of cocatalyst has not affected on the melt flow index.

Figure 3 shows the kinetic profiles of ethylene polymerization using TEA, TEA + DEAC, and TEA + EADC cocatalysts under the same polymerization conditions. According to the diagrams, the polymerization kinetic in the presence of TEA, TEA + DEAC, and TEA + EADC in three molar ratios of 90/10, 85/15, and 80/20 was build up type. In fact, the activity profiles were almost identical. It reveals that the presence of Cl-containing cocatalysts changed the absolute activity (area under the surface of curves), without alteration of activation and deactivation trend. It was corresponded to the lower molar ratio of

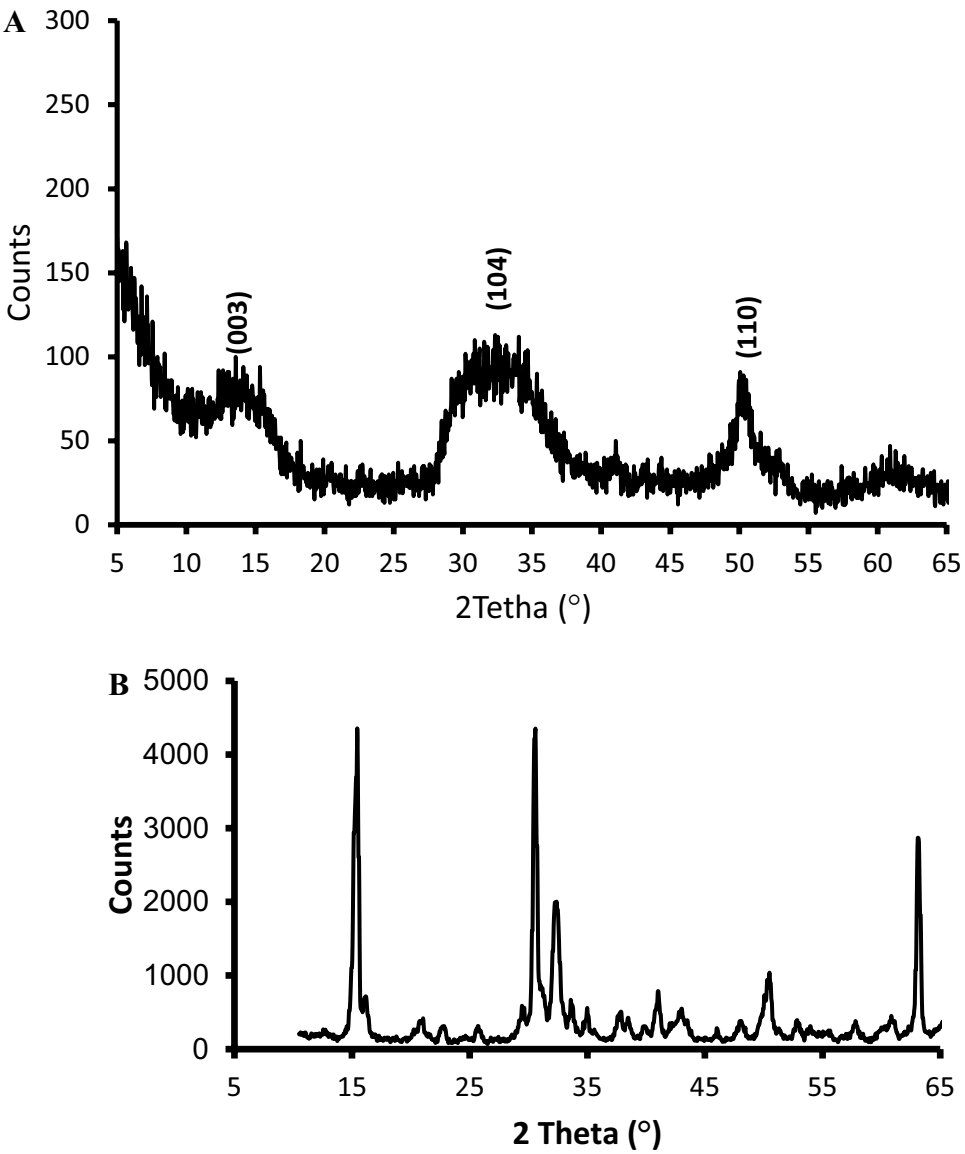

Fig. 2 XRD pattern of the **A** employed catalyst and **B** neat $MgCl_2$

Cl-containing cocatlysts (maximum 20%) in the cocatalyst composition. Here, in line with activity results, TEA followed by TEA/DEAC (90/10), had the biggest area under the surface of kinetic curves.

Figure 4 exhibits the kinetics of ethylene polymerization in the presence of TIBA and its combination with DEAC and EADC in different ratios of 90/10, 85/15 and 80/20. By comparing Figs. 3 and 4, it can be deduced that the polymerization kinetics in the presence of TEA containing compositions was almost build up, while in the presence of TIBA and related compositions, a decay type polymerization behavior was identified. This can be attributed to the less bulkiness of TEA (it is discussed in the molecular modeling section) which facilitates its effusion into the small cavities, where Ti centers are located. Therefore, it can be said that in an ethylene polymerization under the same condition, TEA will have a higher alkylation ability and consequently a higher polymerization rate compared to TIBA, due to the small size of ethyl groups.

Molecular modeling results

To elucidate the role of $MgCl_2$ surface on chain propagation and termination mechanisms, DFT simulations has been performed. In particular, the (104) and (110) surfaces have been investigated, considering XRD pattern of employed catalyst which revealed domination of these lateral cuts.

Prior to investigate the role of cocatalysts on the ethylene polymerization kinetics, the reaction mechanism has been computed without considering the possible effect of the cocatalysts. The (110) and (104) surfaces may represent different catalytic behaviour in terms of ethylene insertion and

Table 2 Ethylene polymerization results using a variety of cocatalysts

Number of Runs	Cocatalyst type	Molar ratio of cocatalysts	Activity (kg polymer/g cat.h)	$MFI_{2.16}$ (g/10 min)	MFI_5 (g/10 min)	$MFI_{21.6}$ (g/10 min)	FRR ($MFI_{21.6}$/MFI_5)
1	TEA	100	4.25 ± 0.15	1.1 ± 0.1	3.1 ± 0.2	29.6 ± 2.0	9.64
2	TEA/DEAC	80/20	3.00 ± 0.10	1.0 ± 0.1	2.8 ± 0.2	25.2 ± 2.1	9.17
3	TEA/DEAC	85/15	3.25 ± 0.10	1.1 ± 0.1	3.0 ± 0.1	27.5 ± 2.1	9.1
4	TEA/DEAC	90/10	3.42 ± 0.12	1.2 ± 0.1	3.4 ± 0.2	32.0 ± 2.2	9.35
5	TEA/EADC	80/20	2.25 ± 0.11	0.7 ± 0.1	2.1 ± 0.1	18.8 ± 1.5	9.14
6	TEA/EADC	85/15	3.00 ± 0.10	1.0 ± 0.1	2.7 ± 0.2	25.0 ± 2.1	9.15
7	TEA/EADC	90/10	2.70 ± 0.09	1.0 ± 0.1	2.6 ± 0.2	24.2 ± 2.0	9.23
8	TIBA	100	3.33 ± 0.08	2.0 ± 0.2	3.2 ± 0.2	29.4 ± 2.0	9.2
9	TIBA/DEAC	80/20	2.51 ± 0.10	1.1 ± 0.1	3.0 ± 0.2	26.7 ± 2.0	8.9
10	TIBA/DEAC	85/15	2.22 ± 0.07	1.0 ± 0.1	2.8 ± 0.2	24.8 ± 1.8	8.8
11	TIBA/DEAC	90/10	3.04 ± 0.12	1.2 ± 0.1	3.3 ± 0.1	28.8 ± 2.0	8.7
12	TIBA/EADC	80/20	2.27 ± 0.07	0.9 ± 0.1	2.7 ± 0.2	23.8 ± 1.7	8.7
13	TIBA/EADC	85/15	3.00 ± 0.10	1.3 ± 0.1	3.7 ± 0.1	32.2 ± 1.9	8.8
14	TIBA/EADC	90/10	3.15 ± 0.09	1.5 ± 0.1	4.3 ± 0.2	38.4 ± 2.1	8.9

Polymerization conditions: PC2: 5 bar, PH2:3 bar, Al/Ti: 200, T: 80 °C, Ptot: 8 bar, t: 2 h, hexane: 650mL

reaction with H_2 as chain transfer agent. In fact, the interaction of $TiCl_4$ with (104) is too weak for the formation of stable grafted species [33]. In addition, it was demonstrated that $TiCl_4$ is more likely coordinated to the (104) surface as dimer or polymer. However, to exclude the probable effect of dimeric structure on the calculated energies, we used monomeric form of $TiCl_4$ on both surfaces. This is the assumption that many other researchers use in their investigations, since the catalytic activity did not show remarkable differences [34, 35]. In fact, computational studies rely on the use of monomeric form of $TiCl_4$ and not dimer or polymeric one [6, 36].

The catalytic pathway starts with the ethylene insertion and followed by the reaction with H_2 molecule, as the well-known chain transfer agent. In detail, the reaction mechanism is based on the neutral pentacoordinate species $TiCl_4Et$ **I** supported on $MgCl_2$ surface, where a thermodynamically favorable ethylene molecule is coordinated, forming the intermediate **II**. Then, the insertion of the olefin substrate in the Ti-C bond implies the first energy barrier, leading to, again, a pentacoordinate Ti specie (**III**). The following step implies the coordination of the hydrogen molecule to the resulting intermediate **III** leading to intermediate **IV**. Actually, this second substrate will allow the hydrogenation of the first carbon attached to the titanium and at the same time the H transfer to the metal, forming the intermediate hydride **V**, together with the release of a butane molecule. All the structures are available on Supplementary Information (Table S1). Going to quantitative results, both surface terminations show practically the same energy barriers for the ethylene insertion and butyl formation as it is depicted in Fig. 5. On (110) surface, the ethylene coordination was 2.3 kcal/mol favored than (104), although the energy barrier for the insertion into the Ti-C bond for (104) termination was 0.6 kcal/mol lower than for (110). The second energy barrier to consider is the H transfer from molecular H_2. As it is shown in Fig. 5, the hydrogen transfer was not the rate determining step (rds) of the reaction on (110) surface, since

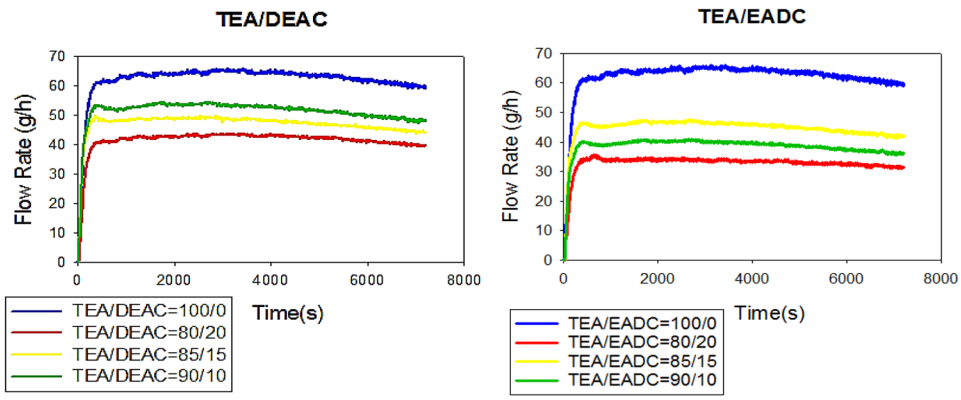

Fig. 3 Rate-time profiles of ethylene polymerization with TEA, TEA + DEAC, TEA + EADC (Polymerization conditions: P_{C2}: 5 bar, P_{H2}:3 bar, Al/Ti: 200 mol/mol, T: 80 °C, P_{tot}: 8.0 bar, t: 2 h, hexane: 650 mL)

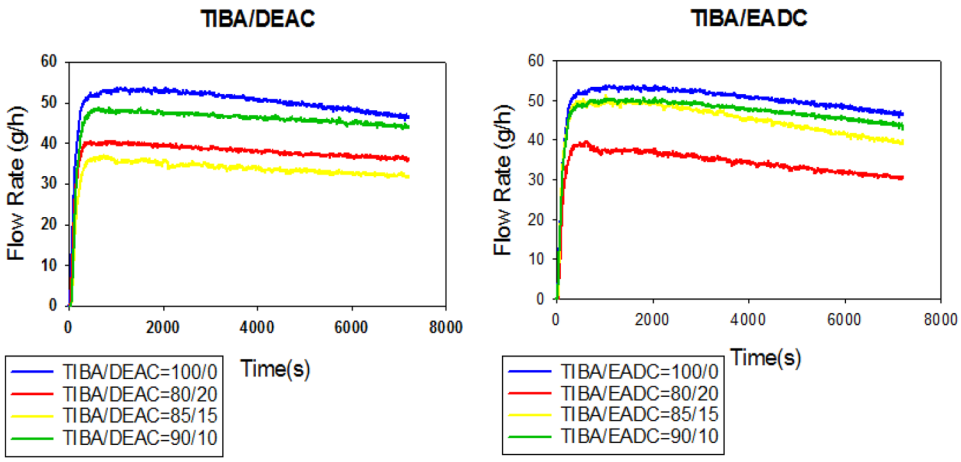

Fig. 4 Rate-time profiles of ethylene polymerization with TIBA, TIBA + DEAC, TIBA + EADC (Polymerization conditions: P_{C2}: 5 bar, P_{H2}:3 bar, Al/Ti: 200 mol/mol, T: 80 °C, P_{tot}: 8.0 bar, t: 2 h, hexane: 650 mL)

the energy barrier was 9.9 kcal/mol, thus, 1.0 kcal/mol lower than the ethylene insertion. The transition state structure depicted on Fig. 6a shows that butyl molecule moves away from the Ti atom while one of the H atoms is bonded to Ti and the other forms the C-H bond with butyl. Similar mechanism was observed for (104) termination although an energy barrier over than 45 kcal/mol was found, discarding a priori the H transfer reaction. Both transition state structures implied the bonding of both hydrogens on Ti as a previous step to eject and hydrogenate the butyl moiety. It has been observed (Fig. 6b) that Ti atom supported on (104) move upwards during the proton transfer reaction, elongating one of the Ti-$Cl_{surface}$ bond around 1 Å and shortening the Ti-$Cl_{cluster}$ bonds (~0.1 Å) to accommodate protons and throw out the butyl moiety (see Fig. 6b). Instead, the Ti-Cl bond elongation was not observed for (110) since the Ti atom did not change the initial position. Furthermore, it is clearly observed that the distance between the H bonded to Ti cluster and the butyl moiety is more than 1 Å larger on (104) surface. These structural differences can explain the large energy difference found by DFT simulations.

According to literature, polymerization rate has a direct relationship with the formation of active centers through alkylation of $TiCl_4$ by the cocatalysts. As a result, each cocatalyst can play a major role in the rate of polymerization due to its unique chemical structure [13]. Considering that $TiCl_4$ catalysts supported on (110) termination is more catalytically active than on (104) cut, the effect of Al complexes in the transalkylation process to insert the ethyl on $TiCl_4$ clusters has been investigated using this particular termination. The preferred choice of (110) termination is not only based on the computational results on bare surface, otherwise it agrees with the recent findings of Taniike-Groppo group which demonstrate that alkylated

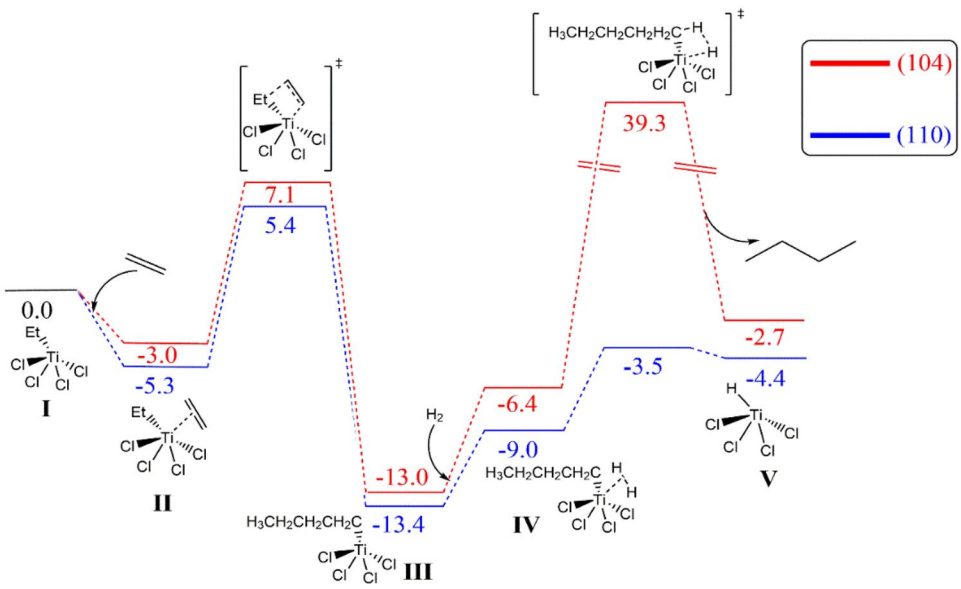

Fig. 5 Reaction profile of ethylene insertion and proton transfer on $TiCl_4$ cluster supported on $MgCl_2$ (104) and (110) surfaces (relative Gibbs energies in kcal/mol)

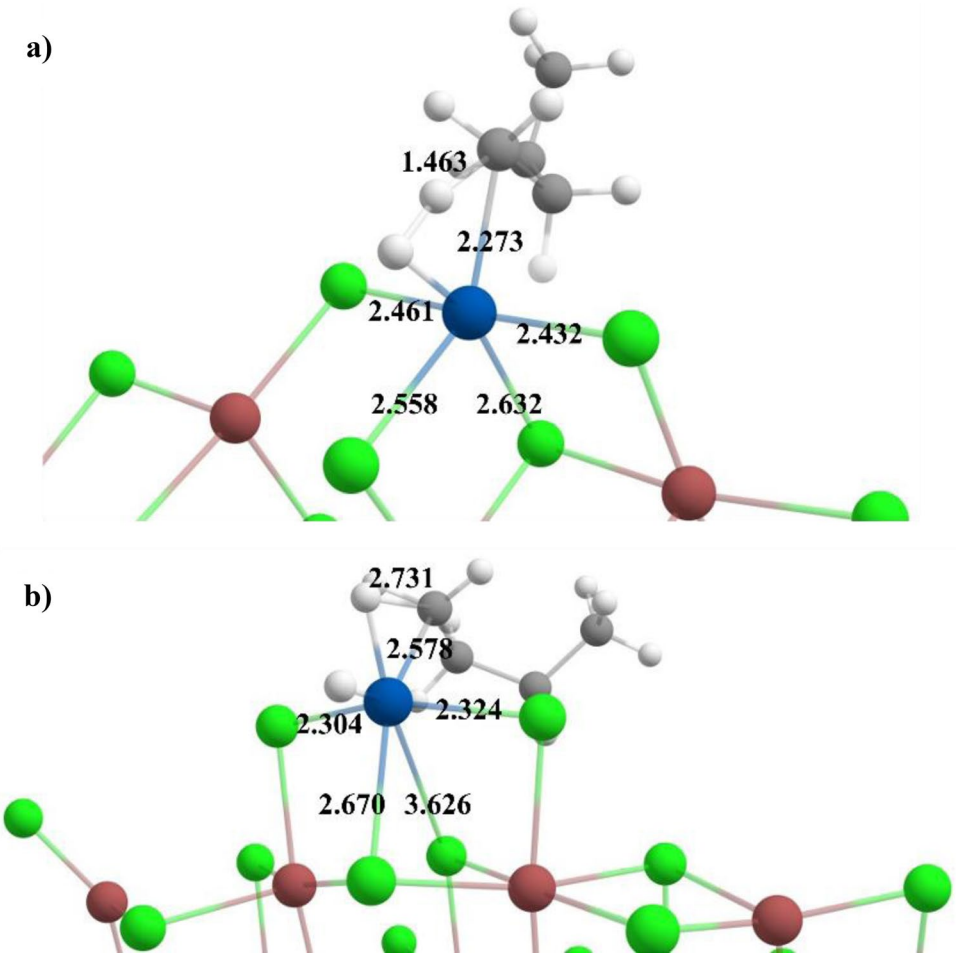

Fig. 6 Transition state **IV-V** for **a** (110) and **b** (104) surfaces (selected distances given in Å)

five-coordinated Ti^{III} centers on (110) termination is mainly involved in ethylene polymerizations using TEA as cocatalyst [37]. The structures have been optimized adsorbing the Al complex on chloride surface atom near to Ti site, as it is exhibited in Fig. 7 for TEA system. This model was selected according to the theory of the role of flexible ancillary ligands in heterogeneous polymerization catalysts [38]. The computed reaction energies indicate that the transalkylation is thermodynamically favored using DEAC, by -5.8 kcal/mol. Although the process using TEAL and EADC was endothermic, by 6.3 and 3.9 kcal/mol, respectively, the unfavorable thermodynamic energy values were relatively low, and thus, the reaction was still possible at room temperature. The use of $\%V_{Bur}$ index, developed by Falivene et al. [39, 40] gives values of 78.7, 80,6, 74.6, and 76.2, for the TEA, TIBA, DEAC, and EADC, Al based systems, respectively. The SambVca code, employed for the calculation of V_{Bur}, calculates the volume of the first sphere around the Ti active center, which is the region where polymerization takes place. The standard radius around the metal is 3.5 Å in these calculations [39, 40]. Thus, the thermodynamic results are directly correlated with the sterical hindrance of the cocatalysts on the surface, and the steric maps in Fig. 8 confirmed this hypothesis [41–43]. Indeed, when the steric hindrance increases, the performance is worse [44, 45]. This fact could explain the lower activity of TIBA containing cocatalysts in comparison to TEA and the decay type of kinetic curves in the experimental section.

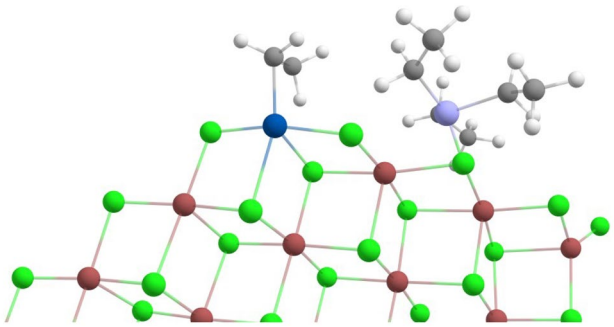

Fig. 7 A schematic representation of the employed $MgCl_2$ (110) model containing TEA as cocatalyst

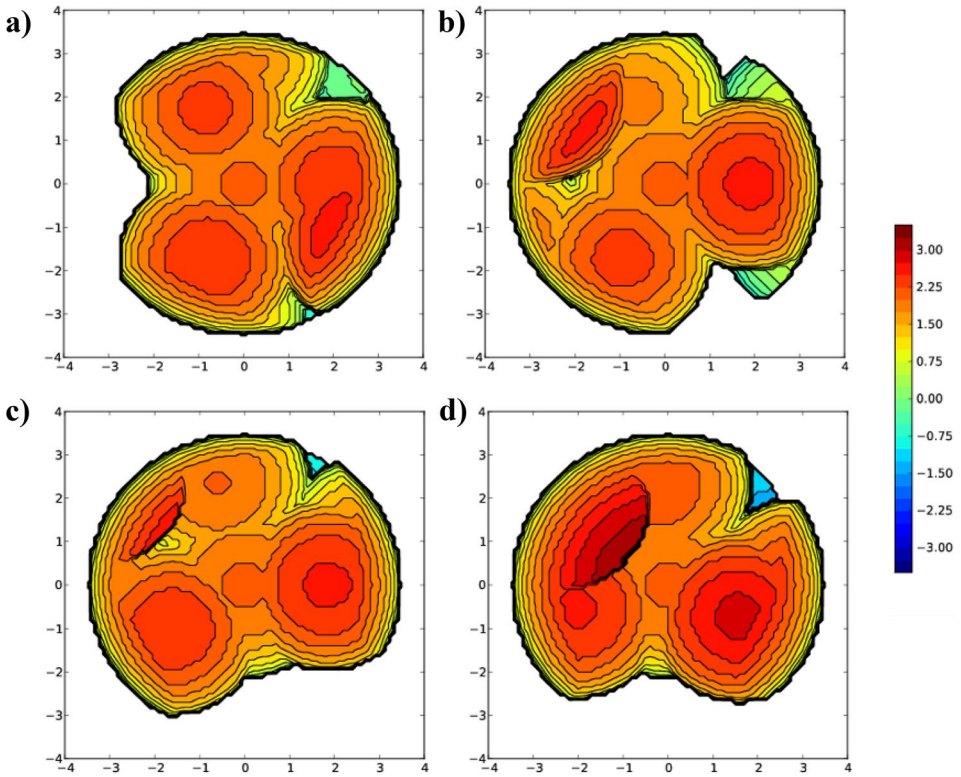

Fig. 8 Steric maps (plane xy) of **a** TEA **b** TIBA, **c** DEAC, and **d** EADC with the linking a-C in the center, Ti in the z axis, and the b-C bonded to Ti on the XZ plane, of the TS **IV-V**, with a radius of 3.5 Å (for the Al based complexes Al was used as the center, the linking Cl in the z axis, and the closest a-C on the X axis)

Finally, the reaction mechanism was computed considering the most favorable cocatalysts according to experimental results (TEA) on (110) surface of $MgCl_2$. With the goal to explore the role of Cl-containing cocatalysts, the reaction mechanism with DEAC and EADC was investigated as well. Table 3 reports the energy barriers for butyl formation (E_b 1) and H transfer (E_b 2). In general, no huge variations on the rate limiting step of the reaction were found in comparison to the energy barriers calculated for the $TiCl_4$ cluster supported on $MgCl_2$ (110) surface. As it can be observed, TEA show the same energy value for the energy barriers, 11 kcal/mol. The DEAC cocatalysts show slightly lower energy barriers (1.4 kcal/mol) with respect to the use of TEA and the calculations without cocatalysts. It is worth mentioning that the energy barrier in ethylene insertion is not correlated to the catalyst activity. In fact, it corresponds to the kinetics of ethylene polymerization. Besides the energy path and energy barrier, other factors influence the polymerization yield such as number of active sites, inherent propagation rate constant, strength of reducing agent, access of the monomers to the metal active center, and the catalyst stability among others. The experimental findings can be related with the low concentration of DEAC, which reduces the probability to be close to Ti sites and the number of active/reduced sites, since one must take into account that TEA is a stronger reduced agent than DEAC. Therefore, our simulations suggest that the use DEAC as main cocatalyst would slightly improve the kinetics of ethylene polymerization. With respect to the EADC, the cocatalysts that contain more chloride ligands, presents the larger barriers. On the other hand, one can hypothesize that cocatalyst may play a most relevant role on $MgCl_2$ (104) termination, where the rate limiting step is higher than 45 kcal/mol. The presence of cocatalyst can stabilize the Ti cluster, avoiding the cluster displacement, and reducing the energy value of the rate limiting step.

Table 3 Gibbs energies (in kcal/mol) of the energy barriers on $MgCl_2$ (110) surface including the Al complexes

	E_b 1 (kcal/mol)	E_b 2 (kcal/mol)
Bare surface	10.7	9.9
TEA	10.9	11.0
DEAC	9.5	9.3
EADC	15.3	18.8

Conclusions

In this paper, the effect of 14 kinds of cocatalyst compositions having different molar ratio of TEA, TIBA, DEAC, and EADC on the catalytic performance of a commercial Ziegler–Natta catalyst was identified. In this regard, considering the molar composition of cocatalysts in industrial plants, TEA and TIBA

were the main component, while DEAC and EADC were used in 10–20 molar percent. Among the studied cocatalyst compositions, TEA, TEA/DEAC (90/10) and TIBA revealed the largest activities, while no considerable effect on polymer MFI was detected. DFT simulations of a model Ziegler–Natta catalyst containing (110) and (104) surfaces unveiled the large energy barrier for the proton transfer process on (104) cut (45.7 kcal/mol) in comparison with the low energy barriers observed for (110) termination (11 kcal/mol, ethylene insertion). The $\%V_{Bur}$ show the higher free volume around TEA in comparison with TIBA, confirming that steric hindrance problems of cocatalysts affects the catalytic activity. Finally, the reaction mechanism computed with TEA, DEAC, and EADC as cocatalyst reveal that EADC decreases the kinetics of the polymerization due to the increase of the energy barriers, and DEAC slightly improve the kinetics of ethylene polymerization.

Supplementary information The online version contains supplementary material available at https://doi.org/10.1007/s10965-022-03050-1.

Acknowledgements S.P.P thank the Spanish Ministerio de Ciencia e Innovacion for Juan de la Cierva Formacion fellowship (FJC2019-039623-I).

Funding Open Access funding provided thanks to the CRUE-CSIC agreement with Springer Nature.

Declarations

Conflicts of interest There are no conflicts to declare.

References

1. Jiang B, Liu X, Weng Y, Fu Z, He A, Fan Z (2019) Mechanistic study on comonomer effect in ethylene/1-hexene copolymerization with $TiCl_4/MgCl_2$ model Ziegler-Natta catalysts. J Catal 369:324–334
2. Jiang B, Weng Y, Zhang S, Zhang Z, Fu Z, Fan Z (2018) Kinetics and mechanism of ethylene polymerization with $TiCl_4/MgCl_2$ model catalysts: Effects of titanium content. J Catal 360:57–65
3. Akram MA, Liu X, Jiang B, Zhang B, Ali A, Fu Z, Fan Z (2021) Effect of alkylaluminum cocatalyst on ethylene/1-hexene copolymerization and active center distribution of $MgCl_2$-supported Ziegler-Natta catalyst. J Macromol Sci Part A 58:539-549
4. Bahri-Laleh N, Correa A, Mehdipour-Ataei S, Arabi H, Haghighi MN, Zohuri G, Cavallo L (2011) Moving up and down the titanium oxidation state in Ziegler–Natta catalysis. Macromolecules 44:778–783
5. Jiang B, Zhang B, Guo Y, Ali A, Guo W, Fu Z, Fan Z (2020) Effects of titanium dispersion state on distribution and reactivity of active centers in propylene polymerization with $MgCl_2$-supported Ziegler-Natta catalysts: A kinetic study based on active center counting. ChemCatChem 12:5140–5148
6. Bahri-Laleh N, Hanifpour A, Mirmohammadi SA, Poater A, Nekoomanesh-Haghighi M, Talarico G, Cavallo L (2018) Computational modeling of heterogeneous Ziegler-Natta catalysts for olefins polymerization. Prog Polym Sci 84:89–114
7. Liu B, Tian Z, Jin Y, Zhao N, Liu B (2018) Effect of alkyl aluminums on ethylene polymerization reactions with a Cr-V bimetallic catalyst. Macromol React Eng 12:1700059
8. Naji-Rad E, Gimferrer M, Bahri-Laleh N, Nekoomanesh-Haghighi M, Jamjah R, Poater A (2018) Exploring basic components effect on the catalytic efficiency of Chevron-Phillips catalyst in ethylene trimerization. Catalysts 8:224
9. Li P, Tu S, Xu T, Fu Z, Fan Z (2014) The influence of combined external donor and combined cocatalyst on propylene polymerization with a $MgCl_2$-supported Ziegler-Natta catalyst in the presence of hydrogen. J Appl Polym Sci 132:41689
10. Hu J, Han B, Shen X-r, Fu Z-s, Fan Z-q (2013) Probing the roles of diethylaluminum chloride in propylene polymerization with $MgCl_2$-supported ziegler-natta catalysts. Chin J Polym Sci 31:583–590
11. Yu Y, McKenna TFL, Boisson C, Lacerda Miranda MS, Martins O (2020) Engineering Poly(ethylene-co-1-butene) through modulating the active species by Alkylaluminum. ACS Catal 10:7216–7229
12. Gharajedaghi S, Mohamadnia Z, Ahmadi E, Marefat M, Pareras G, Simon S, Poater A, Bahri-Laleh N (2021) Experimental and DFT study on titanium-based half-sandwich metallocene catalysts and their application for production of 1-hexene from ethylene. Mol Catal 509:111636
13. Trivedi PM, Gupta VK (2021) Progress in $MgCl_2$ supported Ziegler-Natta catalyzed polyolefin products and applications. J Polym Res 28:13–18
14. Senso N, Praserthdam P, Jongsomjit B, Taniike T, Terano M (2011) Effects of Ti oxidation state on ethylene, 1-hexene comonomer polymerization by $MgCl_2$-supported Ziegler-Natta catalysts. Polym Bull 67:1979–1989
15. Rahmatiyan S, Bahri-Laleh N, Hanifpour A, Nekoomanesh-Haghighi M (2019) Different behaviors of metallocene and Ziegler-Natta catalysts in ethylene/1,5-hexadiene copolymerization. Polym Int 68:94–101
16. Bazvand R, Bahri-Laleh N, Nekoomanesh M, Abedini H (2015) Highly efficient $FeCl_3$ doped $Mg(OEt)_2/TiCl_4$-based Ziegler-Natta catalysts for ethylene polymerization. Des Monomers Polym 18:599–610
17. Gnanakumar ES, Gowda RR, Kunjir S, Ajithkumar TG, Rajamohanan PR, Chakraborty D, Gopinath CS (2013) $MgCl_2{\cdot}6CH_3OH$: A simple molecular adduct and its influence as a porous support for olefin polymerization. ACS Catal 3:303–311
18. Wada T, Funako T, Chammingkwan P, Thakur A, Matta A, Terano M, Taniike T (2020) Structure-performance relationship of $Mg(OEt)_2$-based Ziegler-Natta catalysts. J Catal 389:525–532
19. Fallah M, Bahri-Laleh N, Didehban K, Poater A (2020) Interaction of common cocatalysts in Ziegler–Natta-catalyzed olefin polymerization. Appl Organomet Chem 34:e5333
20. Thakur A, Chammingkwan P, Wada T, Onishi R, Kamimura W, Seenivasan K, Terano M, Taniike T (2021) Solution-state NMR study of organic components of industrial Ziegler-Natta catalysts: Effect of by-products on catalyst performance. Appl Catal A Gen 611:117971
21. Trischler H, Schöfberger W, Paulik C (2013) Influence of alkylaluminum co-catalysts on $TiCl_4$ transalkylation and formation of

active Centers C* in Ziegler-Natta catalysts. Macromol React Eng 7:146–154
22. Kaminsky W, Taniike T, Terano M (2013) The use of donors to increase the isotacticity of polypropylene. In: Polyolefins: 50 years after Ziegler and Natta I, Ed., Springer, Berlin Heidelberg, p 81–97
23. Senso N, Khaubunsongserm S, Jongsomjit B, Praserthdam P (2010) The influence of mixed activators on ethylene polymerization and ethylene/1-hexene copolymerization with silica-supported Ziegler-Natta catalyst. Molecules 15:9323–9339
24. Frisch MJ, Trucks GW, Schlegel HB, Scuseria GE, Robb MA, Cheeseman JR, Scalmani T, Barone V, Petersson GA, Nakatsuji H, Li X, Caricato M, Marenich AV, Bloino J, Janesko BG, Gomperts R, Mennucci B, Hratchian HP, Ortiz JV, Izmaylov AF, Sonnenberg JL, Williams-Young D, Ding F, Lipparini F, Egidi F, Goings J, Peng B, Petrone A, Henderson T, Ranasinghe D, Zakrzewski VG, Gao J, Rega N, Zheng G, Liang W, Hada M, Ehara M, Toyota K, Fukuda R, Hasegawa J, Ishida M, Nakajima T, Honda Y, Kitao O, Nakai H, Vreven T, Throssell K, Montgomery JAJ, Peralta JE, Ogliaro F, Bearpark MJ, Heyd JJ, Brothers EN, Kudin KN, Staroverov VN, Keith TA, Kobayashi R, Normand J, Raghavachari K, Rendell AP, Burant JC, Iyengar SS, Tomasi J, Cossi M, Millam JM, Klene M, Adamo C, Cammi R, Ochterski JW, Martin RL, Morokuma K, Farkas O, Foresman JB, Fox DJ (2016) Gaussian 16, Revision C01, Gaussian, Inc, Wallingford CT
25. Becke AD (1988) Density-functional exchange-energy approximation with correct asymptotic behavior. Phys Rev A 38:3098–3100
26. Perdew JP (1986) Density-functional approximation for the correlation energy of the inhomogeneous electron gas. Phys Rev B 33:8822–8824
27. Grimme S, Antony J, Ehrlich S, Krieg H (2010) A consistent and accurate ab initio parametrization of density functional dispersion correction (DFT-D) for the 94 elements H-Pu. J Chem Phys 132:154104
28. Weigend F, Ahlrichs R (2005) Balanced basis sets of split valence, triple zeta valence and quadruple zeta valence quality for H to Rn: Design and assessment of accuracy. Phys Chem Chem Phys 7:3297–3305
29. Weigend F (2006) Accurate Coulomb-fitting basis sets for H to Rn. Phys Chem Chem Phys 8:1057–1065
30. Ghasemi Hamedani N, Arabi H, Poorsank F (2020) Towards the design of a mixture of diether and succinate as an internal donor in a $MgCl_2$-supported Ziegler-Natta catalyst. New J Chem 44:15758–15768
31. Wada T, Takasao G, Piovano A, D'Amore M, Thakur A, Chammingkwan P, Bruzzese PC, Terano M, Civalleri B, Bordiga S, Groppo E, Taniike T (2020) Revisiting the identity of δ-$MgCl_2$: Part I. Structural disorder studied by synchrotron X-ray total scattering. J Catal 385:76–86
32. Hadian N, Hakim S, Nekoomanesh -Haghighi M, bahri-Laleh N, (2014) Storage time effect on dynamic structure of $MgCl_2$.nEtOH adducts in heterogeneous Ziegler-Natta catalysts. Polyolefins J 1:33–41
33. D'Amore M, Credendino R, Budzelaar PHM, Causá M, Busico V (2012) A periodic hybrid DFT approach (including dispersion) to $MgCl_2$-supported Ziegler-Natta catalysts – 1: $TiCl_4$ adsorption on MgCl2 crystal surfaces. J Catal 286:103–110
34. Piovano A, D'Amore M, Thushara KS, Groppo E (2018) Sprectroscopic evindences for $TiCl_4$/donor complexes on the surfaces of $MgCl_2$-supported Ziegler-Natta catalysts. J Phys Chem C 122:5615–5626
35. D'Amore M, Taniike T, Terano M, Ferrari AM (2022) Effect of internal donors on Raman and Ir spectroscopic fingerprints of $MgCl_2$/$TiCl_4$ nanoclusters determined by machine learning and DFT. Materials 15:909
36. Kumawat J, Gupta VK (2020) Fundamental aspects of heterogeneous Ziegler-Natta olefin polymerization catalysis: an experimental and computational overview. Polym Chem 11:6107–6128
37. Piovano A, Signorile M, Braglia L, Torelli P, Martini A, Wada T, Takasao G, Taniike T, Groppo E (2021) Electronic properties of Ti sites in Ziegler-Natta catalysts. ACS Catal 11:9949–9961
38. Piovano A, Groppo E (2022) Flexible ligands in heterogeneous catalysts for olefin polymerization: Insights from spectroscopy. Coord Chem Rev 451:214258
39. Falivene L, Credendino R, Poater A, Petta A, Serra L, Oliva R, Scarano V, Cavallo L (2016) SambVca 2. A web tool for analyzing catalytic pockets with topographic steric maps. Organometallics 35:2286–2293
40. Falivene L, Cao Z, Petta A, Serra L, Poater A, Oliva R, Scarano V, Cavallo L (2019) Towards the online computer-aided design of catalytic pockets. Nat Chem 11:872–879
41. Poater A, Cavallo L (2009) Comparing families of olefin polymerization precatalysts using the percentage of buried volume. Dalton Trans 0:8885–8890
42. Jacobsen H, Correa A, Poater A, Costabile C, Cavallo L (2008) Understanding the M-(NHC) (NHC = N-heterocyclic carbene) bond. Coord Chem Rev 253:687–703
43. Bahri-Laleh N, Poater A, Cavallo L, Mirmohammadi SA (2014) Exploring the mechanism of Grignard metathesis polymerization of 3-alkylthiophenes. Dalton Trans 43:15143–15150
44. Kaur S, Kumar V, Chawla M, Cavallo L, Poater A, Upadhyay N (2017) Pesticides curbing soil fertility: effect of complexation of free metal ions. Front Chem 5:43–43
45. Tomasini M, Duran J, Simon S, Azofra LM, Poater A (2021) Towards mild conditions by predictive catalysis via sterics in the Ru-catalyzed hydrogenation of thioesters. Mol Catal 510:111692